PASTE DEVELOPMENT FOR ELECTROCHEMICAL SCREEN PRINTING TO STRUCTURE METAL LAYERS OF BACK CONTACT SOLAR CELLS

Gensowski Katharina, Kamp Mathias, Efinger Raphael, Klawitter Markus, Pospischil Maximilian, Eckert Jonas, Bartsch Jonas
Fraunhofer Institute for Solar Energy Systems ISE, Heidenhofstraße 2, 79110 Freiburg, Germany
Phone: +49 (0) 761/45 88-2083
katharina.gensowski@ise.fraunhofer.de

ABSTRACT: An electrochemical etching process is developed to realize the contact pattern of back contact solar cells. It combines ECM technology (Electrochemical Machining) with screen printing to allow local removal of metallic layers for maskless formation of electrically isolated conductive paths. The present work focused on water-based paste development for this application. A plain sodium nitrate solution is used as electrolyte which allows electrochemical etching. Thickener and rheological additives are added to form a screen-printable paste. Additionally different additives are varied to improve printing paste behavior and printing results. The homogeneity of the printing paste is a major factor in the quality of etched structures. The multi-level homogenizing process developed in the present work reduces the particle size by about 35%. Using the optimized $NaNO_3$-based paste, etched lines are formed in 100 nm aluminum layers by the Electrochemical Screen Printing (ESP) process. The smallest lines show widths of 80 µm and the adjacent aluminum regions are electrically separated up to a resistance of 1.6 MΩ. The process time is less than 2 seconds for 156x156 mm^2 samples. Further process modifications ensure another particle size reduction of 33%. First IBC test structures are etched with line widths of 160 µm by using the novel process.
Keywords: printing paste, screen printing, electrochemical etching, IBC solar cell

1 INTRODUCTION

The highest efficiencies of silicon solar cells are reached with a back contact cell design. A heterojunction back contact solar cell fabricated by Kaneka achieves an efficiency of 26.7% [1]. Still, the process complexity, e.g. the metallization, and the high production costs limit back contact solar cells to relatively low production volumes. Possibilities to lower the production costs of high-efficiency back contact solar cells are described by NREL [2]. To use low-cost and simple metallization techniques to produce back contact solar cells is one promising option. Fig. 1 illustrates the difference in process steps between the patented SunPower back end processing route (left) and an alternative route based on electrochemical etching which replaces three costly process steps. Local electrochemical etching is a simple and low-priced method to structure metal layers. Within the present work, electrochemical etching is realized by the Electrochemical Screen Printing (ESP) approach.

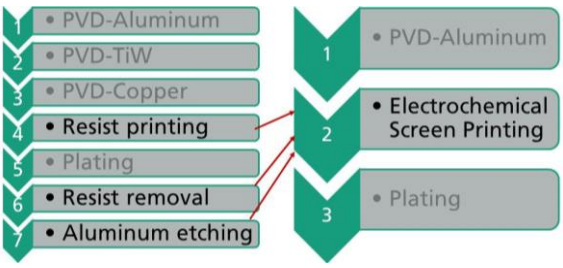

Figure 1: Metallization of IBC solar cells – comparison of the process steps between patented SunPower back end processing route [3] and alternative processing route (ESP) [3–5]

The principle of the Electrochemical Screen Printing is explained in [5, 6]. ESP allows to structure metal layers and generates conductive path structures in these layers e.g. for metallization of solar cells, of circuit boards or electrical sensors. It is a simple, one-step-process. Short process durations and excellent etching control by applied current are its advantages. Optimized commercial printing pastes are not available for the ESP process until now, but the printing paste has a big influence on the process result. Therefore, an optimal printing paste is needed for highest quality of metal structuring. Some requirements and challenges for optimized electrochemical printing pastes for the ESP resemble those of ink systems for other applications described in literature, such as those of Stüwe et al. [7] for inkjet technology to etch metal layers. Still, the processes differ importantly in many aspects. In this work the development and optimization of printing pastes for the ESP are presented.

2 APPROACH AND THEORY

2.1 Electrochemical Screen Printing

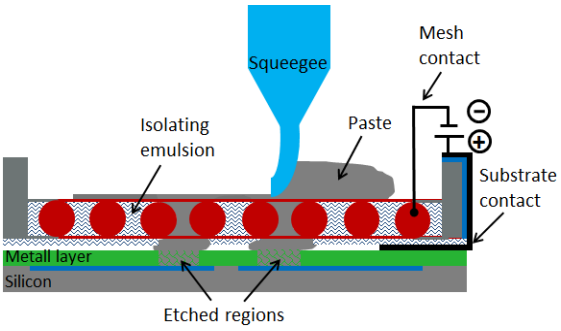

Figure 2: Schematic depiction of the Electrochemical Screen Printing (ESP) process during printing and etching [8]

The ESP, which was developed at Fraunhofer ISE, combines screen printing and electrochemical etching to structure thin metal layers like aluminum, copper and nickel. Fig. 2 depicts the ESP process while printing. The screen, a stainless steel mesh, is coated with an insulating emulsion and functions as cathode. During the printing process, the screen emulsion touches the silicon-wafer

coated with the PVD metal layer, which represents the anode. The squeegee transfers the conductive printing paste onto the metal surface. Thus, the current circuit gets closed and the metal layer will be etched at the printed positions [5, 6].

2.2 Electrochemical printing pastes

Printing pastes for electrochemical etching should possess high etching speed (current proportional to etching rate at similar current efficiency) and satisfactory printing properties (depending on printing techniques), which include rheological properties, paste homogeneity and wettability. Other requirements are high electrical conductivity and aging behavior. A simple and non-toxic paste should be developed to achieve the requirements of conductive printing pastes. The electrochemical printing fluids are water-based systems which need to feature at least an electrolyte of such as sodium nitrate, sodium chloride or sulfuric acid and a rheology modifier. In addition, additives such as wetting agents and foam suppressors can be added to improve the performance.

It is well-known that $NaNO_3$ solution is able to etch metals electrochemically, e.g. as electrolyte for the ECM technology [9–11]. To perform the etching locally, it is necessary to restrict paste spreading by increasing the viscosity and yield point. In terms of sodium nitrate, sodium chloride or sulfuric acid electrolyte, the associated reactions may differ between dissolution of the metal and transformation of metal. $NaNO_3$ and NaCl will dissolve aluminum while H_2SO_4 is especially suited for aluminum treatment, transforming it into anodic aluminum oxide (AAO). AAO is non-conductive and will electrically isolate metal regions from each other [5, 12]. The present work focused on $NaNO_3$ to increase the conductivity of water which functions as solvent. The main reactions which take place at the cathode and at the anode during ESP are the following:

Cathodic: $2\ H_2O + 2e^- \rightarrow H_2\uparrow + 2\ OH^-$

$NO_3^- + H_2O + 2e^- \rightarrow NO_2^- + 2\ OH^-$

Anodic: $2\ Al \rightarrow 2\ Al^{3+} + 6\ e^-$

Overall: $2\ Al + 6\ H_2O \rightarrow 2\ Al^{3+} + 6\ OH^- + 6\ H_2\uparrow$

3 EXPERIMENTAL DETAILS

3.1 Production, homogenizing and characterization of electrochemical printing pastes

The electrochemical printing pastes are prepared in a beaker by using a stirrer to solve the solid components. As is commonly known in paste manufacturing, homogenization of paste is a crucial aspect, and different processing options such as ultrasonic agitation, three roll milling and filtration can be employed. Often, combinations of the mentioned techniques are needed for an optimal result. After stirring the $NaNO_3$-based fluids, they are homogenized by utilizing a multistage process which consists of ultrasonic treatments, a three-level roller mill processing and a two-stage filter processing. The aim is to generate a homogenous paste with small particles, without agglomerates and without air inclusions.

To define the optimal concentration of the paste ingredients a designed experiment was applied. The following four factors were analyzed:

1. Different concentrations of $NaNO_3$ solution
2. Soluble thickeners – thickener 1 (ST1) und thickener 2 (ST2) with a constant concentration
3. Different concentrations of insoluble, particle-based thickener (IPBT)
4. Different concentrations of liquid rheology modifier for thixotropic paste properties (LRM)

Different temperatures of the $NaNO_3$ solution are necessary to solve the thickener completely and more easily – 75°C for soluble thickener ST1, 40°C for the soluble thickener ST2. 48 pastes variations result from the designed experiment.

Moreover additives like humectants and foam suppressors were added to printing pastes. A humectant should improve the duration till the pastes dry out in the screen meshes and the storage life. A foam suppressor should reduce the air bubbles in the paste, so the paste layer shows no interruptions.

The printing pastes are characterized concerning rheological properties, wettability, homogeneity, printability and storage life. The rheological properties, yield point and viscosity, are determined by the rotational rheometer Anton Paar MCR 502 with a two plate rotational geometry. LS13 320 Laser Diffraction Particle Size Analyzer from Beckman Coulter is applied to measure the particle size and distribution of the printing pastes.

To reduce the particle size even more, additional processes are tested. One possibility is to add a dispersant to the printing pastes. Another option is to change the roller distances of the three-level roller mill or to use thinner membranes during the filtration process (see chapter 4.1.2).

3.2 Electrochemical Screen Printing

The ESP process is demonstrated by using monocrystalline silicon wafers with a PVD aluminum layer on top. A stack of silicon-oxide and silicon nitride separates substrate material and metal layer, enabling the measurement of electrical separation. 100 nm und 250 nm aluminum layers are used. For the ESP process a commercial ASYS EKRA screen printing machine S5 STA, which is modified for electrochemical printing, is used.

Depending on the used screens, the mesh widths differ. In the present work, pastes with particle sizes of below 5 µm should obtain process reliable printing results. Also the paste layers, which can be reached, depend on the utilized screen.

4 RESULTS AND DISCUSION

4.1 Electrochemical printing pastes and characterization

To create the first generation paste several rheology modifiers were explored. Thickener ST1 and thickener ST2 resulted in each case in an elastic paste, while the thickener IPBT leads to a waxy consistency with solid agglomerates. The printing fluids which were thickened with only one thickener, did not exhibit the right consistency to use for ESP. Thickener ST2 forms smaller networks than thickener ST1. A combination of two thickeners, thickener ST1 and thickener IPBT or thickener ST2 and thickener IPBT, improved the rheological properties of the medium. Additionally the printability of the paste is optimized with another additive, the modifier LRM. This rheology modifier changes the thixotropic flow behavior of the medium and builds a three-dimensional molecular network configuration, thus increasing the stability under load.

4.1.1 Results of designed experiment

In the next step the paste mixture is optimized by using a designed experiment and by developing a multilevel homogenizing process. 20% $NaNO_3$ solution thickened with thickener ST2 works well. Higher concentrated $NaNO_3$ solution and thickener ST2 result in inhomogeneous pastes. By using thickener ST1 in 20% to 40% $NaNO_3$ solution, the viscosity of the medium increased without any flocculation. In addition, the multi-stage homogeneity process worked well with thickener ST1-based paste.

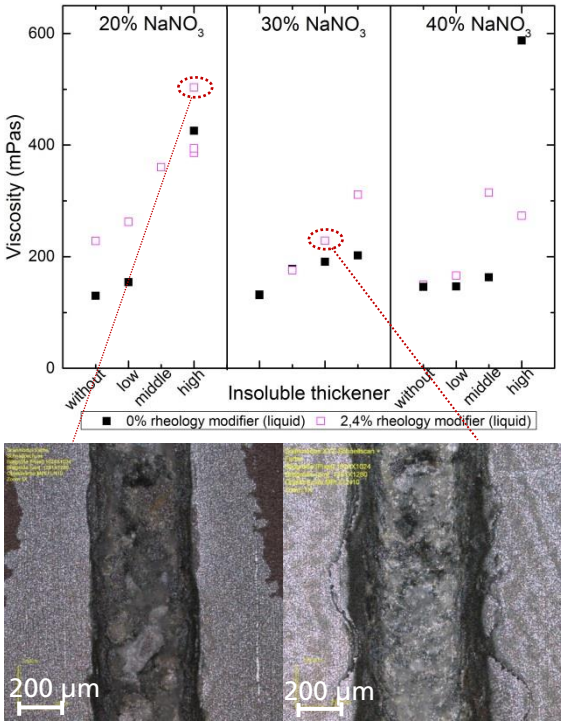

Figure 3: Diagram: viscosity values at shear rate of 100 s^{-1} of thickener ST1 thickened printing fluids at different concentration levels; microscope images: two printing results for two different printing pastes (screen opening: 300 µm)

The viscosity of printing fluids depends on the concentration and combination of the additives (Fig. 3). Thickener ST1 combined with the three different concentrated $NaNO_3$ solutions gives very similar viscosities; about 130 mPas at shear rate of 100 s^{-1}. Thickener IPBT generates a viscosity increase depending on the concentration. If high level of thickener IPBT is added to the thickener ST1 based 20% $NaNO_3$ solution, the viscosity is 426 mPas at 100 s^{-1}. Furthermore, the viscosity increases also with the modifier LRM. The effect of the rheology additives are lower in a higher concentrated $NaNO_3$ medium compared with the 20% $NaNO_3$ solution.

The two images of etching lines in Fig. 3 visualize that different rheological properties of fluids resulted in different etching widths. The etched line on the left is narrower (428 µm) than the structure on the right (616 µm). The reason for the various line widths is that the used paste for the thinner structure is more viscous (503 mPas) than the utilized fluid on the right (229 mPas), but also the contact angles show differences. As expected the paste spreading is less with a more viscous electrochemical printing fluid.

Most of the printing pastes have got a particle size between 40 µm and 90 µm (d_{90}-value) (Fig. 4). The particles are too large, thus the huge particles clog the screen meshes during the ESP process. The metal surface won't be covered with fluid and no electrochemical reaction will take place. To dispense a paste on an aluminum layer, the measured contact angle is between 75° and 85°. The contact angle should ideally be about 90°, so the paste does not spread and narrow structures can be etched.

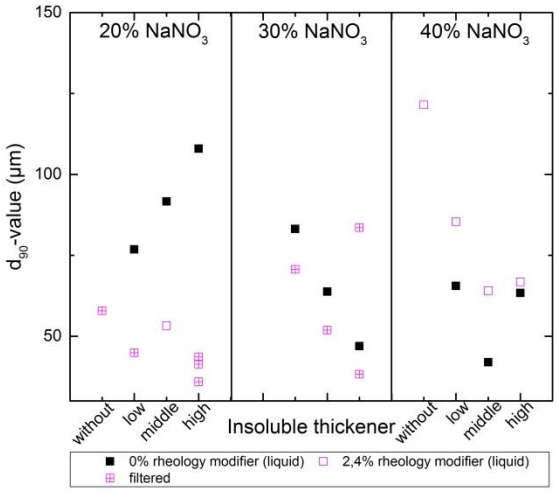

Figure 4: Particle sizes of thickener ST1 thickened printing fluids (different concentration levels of additives)

After characterizing the printing pastes from the designed experiment a standard recipe could be identified. The 20% $NaNO_3$ solution is thickened with low level of thickener ST1. High level of thickener IPBT and high level of modifier LRM are also added. This printing paste has got a viscosity of 503 mPas (shear rate 100 s^{-1}) and a contact angle on aluminum layer of 84°. The particle size, d_{90}-value, is 36 µm. It is possible to store the paste for 30 days without any properties changing.

4.1.2 Further optimization of standard paste

As already mentioned the particle size of printing fluids could be minimized from 47 µm to 30 µm (d_{90}-values), which corresponds to a reduction of about 35% (first generation printing pastes). It is expected that the breakup of agglomerates is one reason for reducing the d_{90}-values. The agglomerates consist of the thickener IPBT, because this additive tends to form agglomerates. The particles of 30 µm or larger are still too big for fine screen meshes. The aim is to create particle size smaller than 5 µm. This is why further optimization of the standard paste from the designed experiment was made.

The first possibility to minimize even more the particle size is to add a dispersing agent to the standard recipe from the designed experiment. The concentration of the dispersant was varied. Fig. 5 depicts the particle distribution of these printing fluids. All printing pastes with dispersant have got significantly smaller particle sizes than the best paste from the designed experiment (d_{90} = 36 µm). The printing fluid with high level of dispersing agent shows the most improved particle distribution because of the border areas. This printing fluid contains very small particles and only few agglomerates in the range of 100 µm to 200 µm. The

precise particle values are presented in Table I.

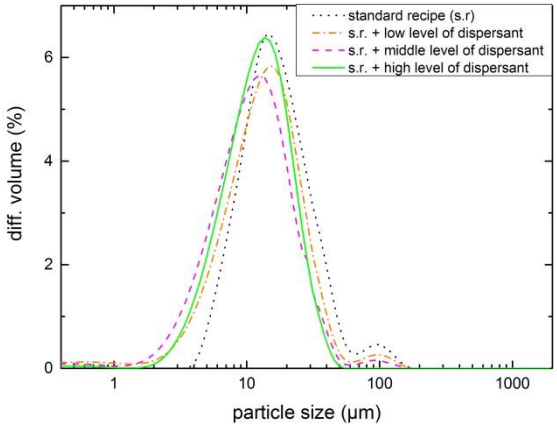

Figure 5: Distribution curves of standard paste from the designed experiment (s.r.) and different concentration of a dispersing agent

Table I: Particle values of standard paste from the designed experiment and different concentration of dispersant

	d_{10} (µm)	d_{50} (µm)	d_{90} (µm)
Standard recipe (s.r.)	8	16	36
S.r. + low level of dispersant	5	13	29
S.r. + middle level of disp.	4	11	25
S.r. + high level of disp.	5	12	24

To influence the particle size the use of the contact mode at the three roll mill is also possible. The mode is controlled by a force value. The distance of the rolls is 0 µm, so the agglomerates are even more broken up. The risk to form flakes during the homogenization process does not exist in this case, because no metal particles are used which might be deformed permanently.

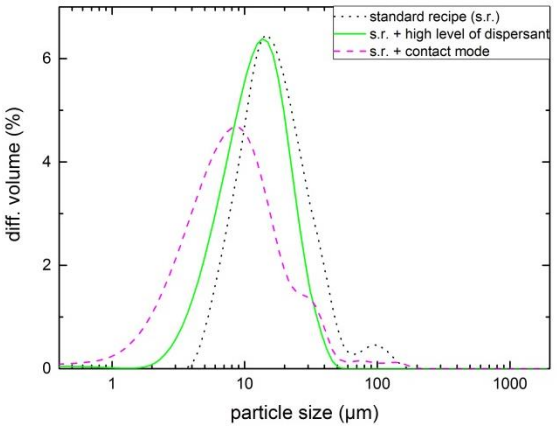

Figure 6: Distribution curves of three different printing pastes – standard printing fluid from designed experiment, printing paste with high level of dispersing agent and printing paste which is homogenized with contact mode

Table II: Particle values of further optimized printing pastes

	d_{10} (µm)	d_{50} (µm)	d_{90} (µm)
Standard recipe	8	16	36
Standard recipe + dispersant	5	12	24
Standard recipe + contact mode	3	8	24

Table II shows the different particle size values of three fluids. One is the best fluid from the designed experiment, one paste contained a dispersant in addition to the standard recipe, in one case the standard paste was run over the three roll mill in contact mode. In comparison to d_{90}-values of the standard recipe, the d_{90}-values of the two improved pastes concerning particle size is significantly smaller. The d_{90}-value is reduced again by about 33%. Both methods to minimize the particle size work well. Fig. 6 depicts the difference in the particle distribution curves of the two homogenization processes. The green, solid curve shows a narrower curve shape that means that the particle size distribution is smaller. The paste is more homogeneous than the printing fluid which associated to the magenta, dashed curve. Additionally, the printing paste with dispersant (green, solid graph) does only exhibit very few agglomerates in the scale of 100 µm to 200 µm. The advantage of the particle distribution of the magenta, dashed curve is that the printing paste has got more really small particles (> 2 µm) than the paste with dispersant.

A third possibility to reduce the particle size is to apply smaller membranes during the filtration. This method lowers the large agglomerates. However, if there are too many large agglomerates left, the membranes are frequently clogged and much paste is lost. In the future these methods of reducing the particle size will be combined.

4.2 Electrochemical Screen Printing

Using the first generation of developed paste, printing processes through screen openings of 50 µm to 100 µm could be realized on PVD-aluminum layers successfully, but with an optimization potential (Fig. 7). The widths of the etched lines were twice as large as the screen openings. Each structure features a length of 28 mm. Another difficulty is also shown in Fig. 7 (red marks). The etched structures exhibit some interruptions, consequently the aluminum regions are not electrically separated. Air bubbles, agglomerates, too thin paste layers and dried out pastes in screen meshes might be reasons. The printing paste has to optimized to achieve improved etched structures. Also, process conditions such as current/voltage characteristics could be adjusted.

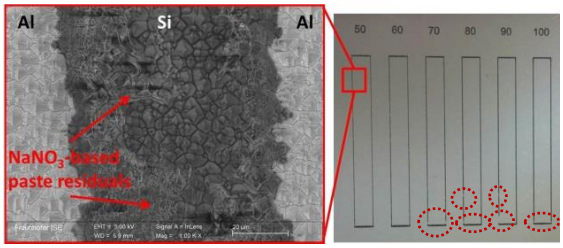

Figure 7: Results of ESP on PVD-Al layer with $NaNO_3$-based paste; Photograph of etched structures with interruptions by using 50 µm to 100 µm screen openings (right); SEM image of etched aluminum and paste residuals by using 50 µm screen opening (left)

A paste from the designed experiment was used to structure a 100 nm aluminum layer (Fig. 8). The printing speed which corresponds to the etching time is 150 mm/s. The aluminum areas are electrically separated (1.6 MΩ) and the line width is around 80 µm for a screen opening of 50 µm. Thus, rheological properties and paste homogeneity of the printing fluids could be optimized, whereby the reached printing results are satisfactory.

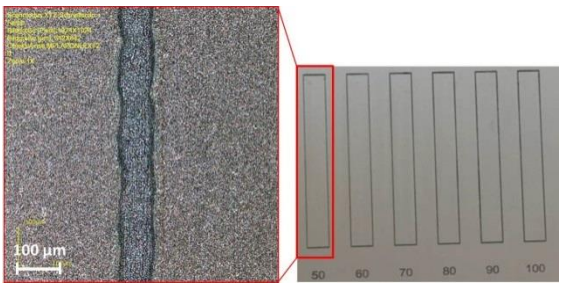

Figure 8: Results of ESP on 100 nm PVD-Al layer with $NaNO_3$-based paste; Photograph of etched structures by using 50 µm to 100 µm screen openings (right); microscope image of etched structure with a line width of 80 µm aluminum achieved with 50 µm screen opening (left)

A paste from the designed experiment was used to structure a 100 nm aluminum layer (Fig. 8). The printing speed which corresponds to the etching time is 150 mm/s. The aluminum areas are electrically separated (1.6 MΩ) and the line width is around 80 µm for a screen opening of 50 µm. Thus, rheological properties and paste homogeneity of the printing fluids could be optimized, whereby the reached printing results are satisfactory.

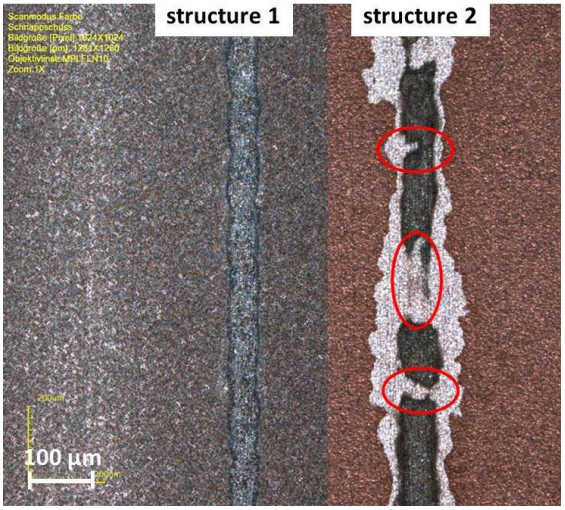

Figure 9: Results of ESP on 100 nm PVD-Al layer with $NaNO_3$-based paste; microscope images of etched structures by using 50 µm screen opening (left: first print experiment; right: second print experiment)

Fig. 9 depicts two different etched lines on aluminum layers. On the left side it is the same structure as shown in Fig. 8. Structure 2 (right) was the next print after structure 1 (left). The results exhibit a big difference, e.g. concerning contour precision, interruptions and therefore electrical separation. The challenge for the future is to create a constant quality of the etched structures between consecutive printing experiments, as in an industrial production several thousand prints have to be performed without any degradation of results. The reason for this behavior has not been fully understood yet. The most likely causes are fast drying of the paste within the screen and clogging of screen meshes by too large particles. The optimization potential is again concerning the printing paste, mainly particle size, drying behavior and paste layer. The particle size should be preferably smaller than 5 µm to reliably pass the typical mesh openings of about 40 µm. In addition, the printing step can be adjusted to flood the screen immediately after printing, thus keeping the paste wet.

The electrochemical printing fluid is an important influencing parameter on the ESP process. In addition, some process parameters affect the quality of etched structures. Fig. 10 depicts several etched lines on aluminum layers created with different printing speeds. The paste spreading can be reduced by using higher printing speeds and more viscous printing pastes. A disadvantage of this might be a shorter reaction time to etch the aluminum completely.

The thicker the aluminum layer, the more challenging is the dissolution of the aluminum. Due to the fact that the paste is consumed by the process it is necessary to transfer enough paste to the metal surface to etch the aluminum completely.

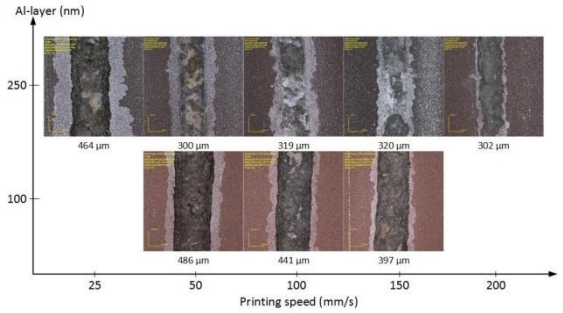

Figure 10: Results of ESP on 100 nm and 250 nm PVD-Al layer with $NaNO_3$-based paste by using different printing speeds

After the ESP process and removal the paste residuals, the etched aluminum layer is plated with a Ni-Cu stack. The processing sequence and SEM images of the plated structures will be published in [8].

Our latest results show the satisfactory structuring of thin aluminum and copper with the ESP process. Further paste improvements are aspired, where a special focus is set on bringing the particle size below 5 µm. Also, the paste transfer behavior will be optimized, to allow structuring of thicker metal layers

Adjusted pastes will also allow higher flexibility towards other processing schemes such as electrochemical dispensing, where the particle size is even more critical.

4.3 First electrochemical screen printed IBC test structure

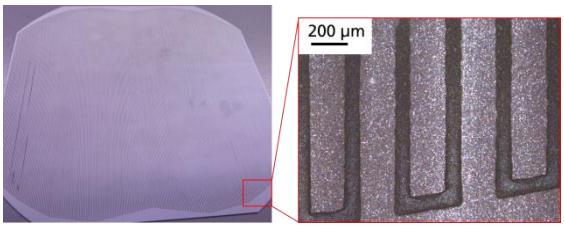

Figure 11: ESP etched IBC test structure on 100 µm PVD-Al layer by using 150 µm screen openings (etched line widths 160 µm)

Fig. 11 illustrates one of the first electrochemical screen printed IBC test structures. The printing duration for the length of 125 mm was 2.5 s. To transfer the process from small test structures to a 125x125 mm² wafer is a challenging task concerning the printing homogeneity, the current distribution and thus the etching

regions. This very first result is considered satisfactory, as it already shows a precise resolution between the different lines and corners.

As already mentioned, the paste has to be improved, but also the current distribution for structuring larger areas has to be optimized. Several approaches to achieve this are currently under investigation. With an improved paste and printing setup, the creating of functional IBC solar cells will be aspired in the future.

5 CONCLUSION

To structure metal layers, a paste for a new etching process (ESP) is developed, with an aspired application in a simplified back contact solar cell back-end process. The simple, first generation $NaNO_3$-based paste consists of thickener ST1, thickener IPBT and rheology modifier LRM. The ESP process was successfully demonstrated on PVD-aluminum layers – line widths of 80 µm are achieved and electrical separation up to 1.6 MΩ is demonstrated. The quality of printing results is not yet similar for repeated printing of the same structure. The aim is to improve the whole etching process (process parameters) and to make the process suitable for high-throughput production.

The first paste mixtures are optimized concerning particle size, rheological properties and printability (etching results) during this work. Also a manufacturing process and a multi-stage homogenization process are developed for printing pastes. For the future there is still a high potential of optimization concerning the homogeneity and composition of printing pastes. First experiments concerning etching IBC test structures are demonstrated. Printing on large area substrates in an industrially relevant speed will be improved.

6 ACKNOWLEDGEMENT

This work was funded by the German Federal Ministry for Economic Affairs and Energy within the project “KAluS50”, grant No. 0324009A.

7 REFERENCES

[1] M. A. Green *et al.*, “Solar cell efficiency tables (version 50),” *Prog. Photovolt: Res. Appl.*, vol. 25, no. 7, pp. 668–676, 2017.

[2] National Renewable Energy Laboratory, *Silicon Materials and Devices R&D | Photovoltaic Research | NREL*. [Online] Available: https://www.nrel.gov/pv/silicon-materials-devices-rd.html. Accessed on: Aug. 09 2017.

[3] W. P. Mulligan, “Solar cell and method of manufacture,” US 7897867 B1.

[4] M. Kamp *et al.*, “Zincate processes for silicon solar cell metallization,” *Solar Energy Materials and Solar Cells*, vol. 120, pp. 332–338, 2014.

[5] M. Kamp *et al.*, “Electrochemical Contact Separation for PVD Aluminum Back Contact Solar Cells,” *Energy Procedia*, vol. 67, pp. 70–75, 2015.

[6] M. Kamp, J. Bartsch, and M. Glatthaar, “Method for structuring layers of oxidizable materials by means of oxidation and substrate having a structured coating,” US20160204699 A1, Aug 18, 2016.

[7] D. Stüwe, D. Mager, D. Biro, and J. G. Korvink, “Inkjet technology for crystalline silicon photovoltaics,” (eng), *Advanced materials (Deerfield Beach, Fla.)*, vol. 27, no. 4, pp. 599–626, 2015.

[8] M. Kamp *et al.*, “Structuring of metal layers by electrochemical screen printing for back contact solar cells: IEEE PVSC, under review,”

[9] M. M. Lohrengel, K. P. Rataj, and T. Münninghoff, “Electrochemical Machining—mechanisms of anodic dissolution,” *Electrochimica Acta*, vol. 201, pp. 348–353, 2016.

[10] K. P. Rajurkar, M. M. Sundaram, and A. P. Malshe, “Review of Electrochemical and Electrodischarge Machining,” *Procedia CIRP*, vol. 6, pp. 13–26, 2013.

[11] S. Wang, Y. Zeng, Y. Liu, and D. Zhu, “Micro wire electrochemical machining with an axial electrolyte flow,” *Int J Adv Manuf Technol*, vol. 63, no. 1-4, pp. 25–32, 2012.

[12] K. Schwirn, “Harte Anodisation von Aluminium mit verdünnter Schwefelsäure: Dissertation,” Zentrum für Ingenieurwissenschaften der Martin-Luther-Universität Halle-Wittenberg, 2008.